SECURITY CLASSIFICATION OF THIS PAGE

REPORT DOCUMENTATION PAGE

1a. REPORT SECURITY CLASSIFICATION Unclassified	1b. RESTRICTIVE MARKINGS None
AD-A221 961 ULE	3. DISTRIBUTION/AVAILABILITY OF REPORT Unlimited
4. PERFORMING ORGANIZATION REPORT NUMBER(S) interium technical report #38	5. MONITORING ORGANIZATION REPORT NUMBER(S)
6a. NAME OF PERFORMING ORGANIZATION Department of Chemistry 6b. OFFICE SYMBOL (If applicable)	7a. NAME OF MONITORING ORGANIZATION Office of Naval Research
6c. ADDRESS (City, State, and ZIP Code) Massachusetts Institute of Technology 77 Mass. Avenue, Bldg. 6-335 Cambridge, MA 02139	7b. ADDRESS (City, State, and ZIP Code) Chemistry Division 800 N. Quincy Street Arlington, VA 22217
8a. NAME OF FUNDING/SPONSORING ORGANIZATION Office of Naval Research 8b. OFFICE SYMBOL (If applicable)	9. PROCUREMENT INSTRUMENT IDENTIFICATION NUMBER N00014-84-K-0553
8c. ADDRESS (City, State, and ZIP Code) Chemistry division 800 N. Quincy Street Arlington, VA 22217	10. SOURCE OF FUNDING NUMBERS PROGRAM ELEMENT NO. / PROJECT NO. / TASK NO. 051-579 / WORK UNIT ACCESSION NO.

11. TITLE (Include Security Classification)
A Viologen/Ruthenium Oxide-Based Microelectrochemical Diode with pH-Dependent...

12. PERSONAL AUTHOR(S) Martin O. Schloh and Mark S. Wrighton

13a. TYPE OF REPORT	13b. TIME COVERED	14. DATE OF REPORT (Year, Month, Day)	15. PAGE COUNT
technical interim	FROM 5/89 TO 5/90	5/16/90	41

16. SUPPLEMENTARY NOTATION
Prepared for publication in the Journal of the American Chemical Society

17. COSATI CODES			18. SUBJECT TERMS (Continue on reverse if necessary and identify by block number)
FIELD	GROUP	SUB-GROUP	viologen microelectrochemical diode, ruthenium oxide

19. ABSTRACT (Continue on reverse if necessary and identify by block number)

See Attached Sheet

20. DISTRIBUTION/AVAILABILITY OF ABSTRACT ☐ UNCLASSIFIED/UNLIMITED ☐ SAME AS RPT. ☐ DTIC USERS	21. ABSTRACT SECURITY CLASSIFICATION Unlimited
22a. NAME OF RESPONSIBLE INDIVIDUAL Mark S. Wrighton	22b. TELEPHONE (Include Area Code) 617-253-1597 / 22c. OFFICE SYMBOL

DD FORM 1473, 84 MAR 83 APR edition may be used until exhausted. All other editions are obsolete.

SECURITY CLASSIFICATION OF THIS PAGE

ABSTRACT

A procedure for selectively derivatizing two adjacent (~1.4 μm apart) microelectrodes (~50 μm long x 2.5 μm wide x ~0.1 μm thick) with RuO_x and the redox polymer derived from hydrolysis of N,N'-*bis*[*p*-(trimethoxysilyl)benzyl]-4,4'-bipyridinium dichloride, $(BPQ^{2+})_n$, to yield a physical $RuO_x/(BPQ^{2+})_n$ junction is reported. Such a junction functions as a pH-dependent diode by virtue of the redox properties of the materials employed. A diode-like current-voltage curve obtains, because charge transport across the $RuO_x/(BPQ^{2+})_n$ junction is effectively unidirectional: the oxidized RuO_x can oxidize the reduced viologen, but the reduced RuO_x cannot reduce the oxidized viologen. The pH dependence arises from the fact that RuO_x has pH-dependent electrochemistry, $E^{0'}$ varies ~71 mV/pH unit from ~+0.42 V vs. SCE at pH = 2 to ~0.0 V vs. SCE at pH = 8, while $(BPQ^{2+})_n$ is a conventional redox polymer with a redox potential ($E^{0'} \approx -0.5$ V vs. SCE) independent of pH. These data are in accord with the pH dependence of the current-voltage curve for the $RuO_x/(BPQ^{2+})_n$-based diode. The magnitude of the diode current at forward bias is determined to be limitied by the charge transport properties of the $(BPQ^{2+})_n$. The current passed through the $RuO_x/(BPQ^{2+})_n$ junction at a fixed applied potential can be modulated repetitively by changing the pH of a flowing stream between pH 4.5 and 8.5.

[Prepared for publication as an article in

Chemistry of Materials]

A Viologen/Ruthenium Oxide-Based Microelectrochemical Diode with pH-Dependent Current-Voltage Characteristics

Martin C. Schloh and Mark S. Wrighton*

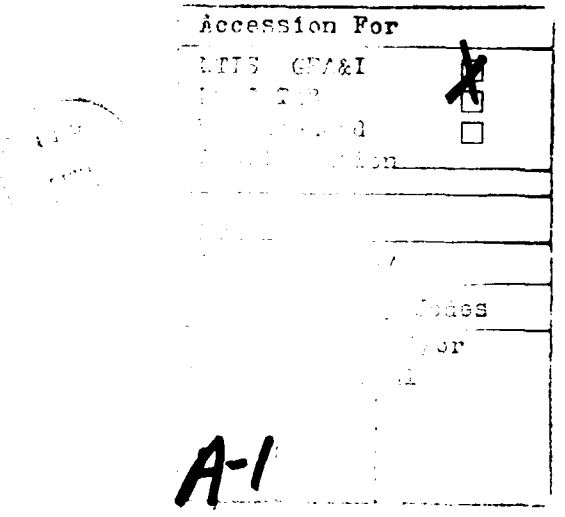

Department of Chemistry

Massachusetts Institute of Technology

Cambridge, Massachusetts 02139

* Address correspondence to this author.

Office of Naval Research

Contract NOOO14-84-K-0553

Task No. 051-597

Technical Report #38

A Viologen/Ruthenium Oxide-Based Microelectrochemical Diode with pH-Dependent Current-Voltage Characteristics

by

Martin O. Schloh and Mark S. Wrighton

Prepared for Publication

in

Journal of the American Chemical Society

Massachusetts Institute of Technology
Department of Chemistry
Cambridge, MA 02139

ABSTRACT

A procedure for selectively derivatizing two adjacent (~1.4 μm apart) microelectrodes (~50 μm long x 2.5 μm wide x ~0.1 μm thick) with RuO_x and the redox polymer derived from hydrolysis of N,N'-*bis*[*p*-(trimethoxysilyl)benzyl]-4,4'-bipyridinium dichloride, $(BPQ^{2+})_n$, to yield a physical $RuO_x/(BPQ^{2+})_n$ junction is reported. Such a junction functions as a pH-dependent diode by virtue of the redox properties of the materials employed. A diode-like current-voltage curve obtains, because charge transport across the $RuO_x/(BPQ^{2+})_n$ junction is effectively unidirectional: the oxidized RuO_x can oxidize the reduced viologen, but the reduced RuO_x cannot reduce the oxidized viologen. The pH dependence arises from the fact that RuO_x has pH-dependent electrochemistry, $E^{0'}$ varies ~71 mV/pH unit from ~+0.42 V vs. SCE at pH = 2 to ~0.0 V vs. SCE at pH = 8, while $(BPQ^{2+})_n$ is a conventional redox polymer with a redox potential ($E^{0'} \approx -0.5$ V vs. SCE) independent of pH. These data are in accord with the pH dependence of the current-voltage curve for the $RuO_x/(BPQ^{2+})_n$-based diode. The magnitude of the diode current at forward bias is determined to be limitied by the charge transport properties of the $(BPQ^{2+})_n$. The current passed through the $RuO_x/(BPQ^{2+})_n$ junction at a fixed applied potential can be modulated repetitively by changing the pH of a flowing stream between pH 4.5 and 8.5.

We wish to report preparation, characterization, and pH response of a microelectrochemical diode based on the selective functionalization of closely spaced (~1.4 μm) Au or Pt microelectrodes (each ~2.5 μm wide, 0.1 μm thick, and ~50 μm long) with RuO_x and a viologen polymer as illustrated in Scheme I. In Scheme I RuO_x is an electro-active, electrodeposited[1] oxide exhibiting a pH-dependent redox potential,[2] and $(BPQ^{2+})_n$ is a redox active polymer derived from hydrolysis of **I** having a redox potential

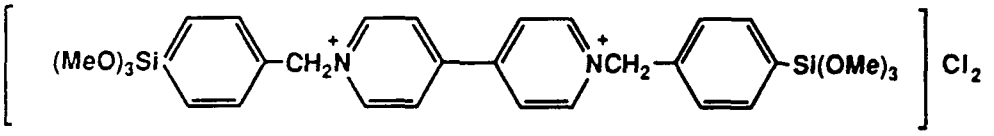

I

independent of pH.[3]

Electrochemical systems of the type shown in Scheme I have previously been shown to behave as diodes in the sense that steady-state current passes in only one direction upon application of a potential across the two electrodes,[4] and a preliminary account of our work on the $RuO_x/(BPQ^{2+})_n$ redox systems has recently appeared.[5] The underlying principles of rectification and redox conduction taking place in such diodes were first demonstrated on sandwich structures of the type metal/redox polymer 1/redox polymer 2/metal by Murray and co-workers.[6] Meyer and his co-workers first published a sandwich bilayer assembly on one electrode having one pH-dependent component,[7] and work from this laboratory has

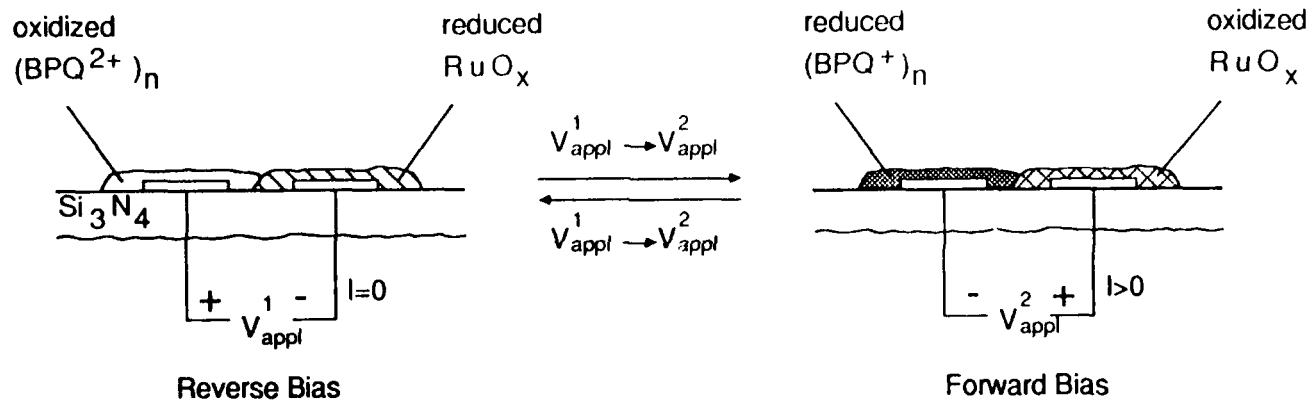

Scheme I. Cross-sectional view of a pH-dependent microelectrochemical diode based on selective functionalization of microelectrodes with RuO_x and $(BPQ^{2+})_n$.

demonstrated a $(BPQ^{2+})_n$/quinone bilayer on one electrode where the quinone is pH-dependent.[8] The system in Scheme I represents the first complete pH-dependent microelectrochemical diode.

Heterojunctions with rectifying behavior in the dry, solid-state have also been made between conducting polymers such as reduced (n-type) and oxidized (p-type) polyacetylene,[9] polyacetylene and polypyrrole,[10] polypyrrole and polythiophene,[11] and polypyrrole and polyaniline.[12] However, in contrast to redox polymer junctions in electrolytes, the electrical properties of these dry conducting polymer heterojunctions are explained in terms similar to those for a classical n-p Si diode.[13]

In general, a microelectrochemical device with a diode-like current-voltage characteristic can be made when (1) the only current path between one electrode to the other is via the redox materials connecting them and (2) the formal potentials, $E^{0'}$, of the two redox materials differ sufficiently such that the redox reaction at the junction of the two redox materials occurs at a fast rate in one direction (downhill) and a slow rate in the other (uphill). Equation (1) and Scheme II summarize the

$$(BPQ^{+})_n + Ru^{IV}O_x \rightleftharpoons (BPQ^{2+})_n + Ru^{III}O_x \qquad (1)$$

thermodynamically favored redox process occurring in the case of our $RuO_x/(BPQ^{2+})_n$-based diode. Taking $E^{0'}$(1) to be

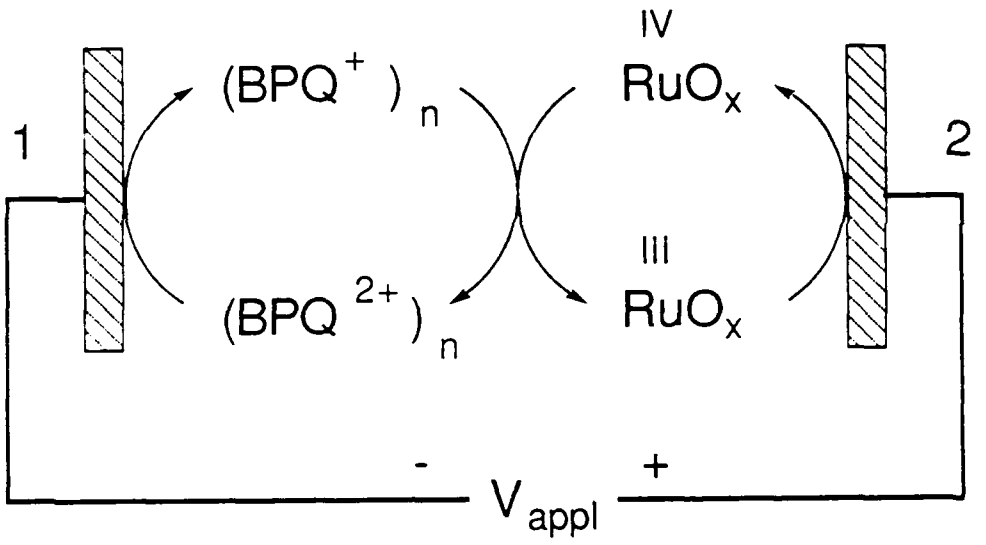

Scheme II. Schematic representation of the redox reaction occurring at the viologen/ruthenium oxide interface when charge is passed between electrode 1 and 2. This is the $RuO_x/(BPQ^{2+})_n$ interface redox chemistry under forward bias, Scheme I.

the formal potential of RuO_x and $E^{0'}(2)$ the formal potential of $(BPQ^{2+})_n$ the difference, $E^{0'}(1)-E^{0'}(2)$, represents the turn-on or threshold potential, V_T, for the microelectrochemical diode. The essential point is that the microelectrochemical device drawn in Scheme I is assembled by bringing a pH dependent redox material, RuO_x, in connection with a redox material, $(BPQ^{2+/+})_n$, which has a pH-independent redox potential. The RuO_x shows a 70 mV/pH positive shift in $E^{0'}$ as pH is lowered,[2] independent of the electrolyte. The result is a microelectrochemical diode with a pH-dependent value of V_T such that V_T is smaller at higher pH.

Experimental

Chemicals. $K_2RuO_4 \cdot 2H_2O$ (Alfa) was used as received and stored in a controlled atmosphere chamber under N_2. N,N'-bis[p-(trimethoxysilyl)benzyl]-4,4'-bipyridinium dichloride, **I**, was synthesized by refluxing a mixture of bipyridine (Aldrich) and *p*-(trimethoxysilyl)benzylchloride (PCR Research Chemicals, Inc.) in CH_3CN following a procedure in the literature.[3]

Electrochemical Equipment. All electrochemical experiments were carried out using a Pine Model RDE4 bipotentiostat and recorded on a Kipp & Zonen BD91 x-y-y' recorder. Where necessary potentials were controlled relative to an aqueous saturated calomel electrode (SCE). Electrochemical measurements were performed under Ar or N_2 at 25 ^{o}C.

Microelectrodes. The Pt or Au microelectrode arrays used in these experiments have been described previously[14] and consist of eight, individually addressable, parallel microelectrodes ~50 μm long, ~2.5 μm wide, and 0.1 μm high with a spacing between the microelectrodes of 1.4 μm. Insulation of the leads to the microelectrodes and encapsulation was afforded by either a manually applied layer of clear epoxy (Hydrosol Division, Dexter Corporation) or a thin Si_3N_4 film, 1.0 μm thick, deposited by Plasma Enhanced Chemical Vapor Deposition, PECVD, and etch-back to the microelectrodes through a mask with a CF_4 plasma etch.

The packaged microelectrode arrays were typically cleaned by a negative potential excursion in 0.1 **M** K_2HPO_4 to

evolve H_2. On some arrays the gap between microelectrodes was narrowed from ~1.1 μm to ~0.3 μm by electrodeposition of Pt or Pd from an aqueous 0.1 **M** K_2HPO_4 solution containing 2 m**M** K_2PtCl_4 or 2 m**M** K_2PdCl_4, respectively. For some of the generation/collection experiments shadow deposited microelectrode arrays were used with interelectrode spacing of ~0.1 μm.[15]

Derivatization of Microelectrodes. RuO_x was deposited from a freshly prepared and deoxygenated 5 m**M** K_2RuO_4/1 **M** NaOH solution.[1,2] The deep orange K_2RuO_4 solution undergoes slow decomposition and/or reduction yielding the formation of a dark green or black amorphous precipitate.[16] A two-compartment cell was used with the counter electrode separated from the working and reference electrode. Selective deposition of RuO_x on one microelectrode was achieved by cycling the electrode potential between -0.2 and -0.8 V vs. SCE at 100 mV/s while holding the potential of adjacent microelectrodes at +0.2 V vs. SCE.[2]

Following the RuO_x deposition, $(BPQ^{2+/+})_n$ can be deposited selectively on an adjacent microelectrode by scanning the electrode potential between 0.0 and -0.75 V vs. SCE at 50 mV/s in an aqueous solution of 0.5 m**M** of **I** and 0.2 **M** KCl/0.1 **M** K_2HPO_4 while holding the adjacent microelectrode at 0.0 V vs. SCE.[3,4] Deposition was allowed to continue until the desired coverage, ~2 x 10^8 mol/cm^2, was achieved. Coverage was determined from the integration of the cyclic voltammetry wave for the $(BPQ^{2+/+})_n$

interconversion at a sweep rate slow enough (<50 mV/s) to fully access all redox active molecules.

pH Variation Experiment. A flowing stream set-up, constructed by joining two chromatography columns filled with buffer solutions of the desired pH, was used to reproducibly give pH variations in the electrolyte stream across the microelectrochemical assembly. The buffer solutions used were 1.0 **M** LiCl or NaCl/0.05 **M** HSO_4^-, acetate, Tris and phosphate for the appropriate pH and were deoxygenated prior to use.

Results and Discussion

a. Cyclic Voltammetry and pH Dependence of $E^{0'}$. The electrochemical deposition of RuO_x is based on the literature procedure[1] and can be accomplished on either Au or Pt microelectrodes.[2] The pH dependent cyclic voltammetry of RuO_x is depicted in Figure 1. In buffered solutions the wave is broad and has been attributed to the Ru^{IV}/Ru^{III} couple.[1] At more positive potentials, the oxidation process overlaps H_2O and Cl^- oxidation giving O_2 and Cl_2 evolution, respectively. Prolonged cycling to the potential of O_2 evolution results in gradual film dissolution. At potentials significantly negative of the $Ru^{IV/III}$ wave, the RuO_x film shows no faradaic activity, but H_2 evolution occurs. H_2 evolution does not affect the $Ru^{IV/III}$ cyclic voltammogram.[2]

The redox potential, $E^{0'}$, for the $Ru^{IV/III}$ redox couple at a specific pH is taken to be the average position of cathodic and anodic current peaks of a cyclic voltammogram. The data obtained for a series of cyclic voltammograms taken in buffered solutions of pH 2.2 to 9.5 are plotted in Figure 2. For comparison the redox potentials for the $(BPQ^{2+/+})_n$ redox polymer couple at different pH's using the same buffers has been included. We find that the redox potential of RuO_x shifts more positive by ~70 mV/pH as the pH is decreased. This type of non-Nernstian pH dependence has also been reported in the voltammetry of other hydrous metal oxides.[17,18] Our earlier work has established that the pH

dependence of the RuO_x is insensitive to a wide range of electrolytes.[2] The redox potential of the $(BPQ^{2+/+})_n$ redox polymer on the other hand, remains constant (also independent of electrolyte)[3] at about -0.5 V vs. SCE as the pH of the solution is changed between 2.2 and 8.5. The $(BPQ^{2+})_n$ system also shows reduction to $(BPQ^0)_n$, but the evolution of H_2 obscures the cyclic voltammetry wave, especially at low pH. Moreover, the $(BPQ^0)_n$ state is much less durable than either the $(BPQ^{2+})_n$ or $(BPQ^+)_n$ states.[3]

b. Generation/Collection Experiments and Relative Charge Transport Properties of RuO_x and $(BPQ^{2+})_n$. Figure 3 illustrates typical data relating to steady-state charge transport properties of RuO_x in aqueous electrolyte media. The data shown relate to an array of eight Pt microelectrodes all coated with RuO_x such that the RuO_x connects the individually addressable microelectrodes. The microelectrodes used are ~0.1 μm apart, to give larger steady-state currents. The actual experiment[19-21] is analogous to a rotating ring disk electrode experiment[22] with a collection efficiency of unity, since the charge carriers are immobilized. There is a steady-state current between so-called generator and collector microelectrodes when the generator electrodes are moved to a potential where RuO_x is oxidized, 0.4 V vs. SCE, while the collector electrodes are held at a potential where RuO_x is reduced, -0.4 V vs. SCE. Under such conditions, the largest possible concentration gradient of reduced and oxidized RuO_x exists,

giving the maximum current which can pass through the material. For the data in Figure 3 every other electrode of an eight-electrode array uniformly coated with RuO_x is used as a generator and the other microelectrodes are collectors. The use of this interdigitated arrangement increases the magnitude of the generator/collector current.

The fact that the generation/collection response for RuO_x-based microelectrodes is the same for all scan rates shown, indicates that oxidation and reduction of the RuO_x is rapid on the timescale of the cyclic voltammetry. The rapid oxidation and reduction, of course, is related to the charge transport/ion diffusion in the RuO_x. The steady-state diffusion coefficient for charge transport, D_{ct}, in RuO_x is proportional to the steady state generation/collection currents in Figure 3. From cyclic voltammetry it can be determined that about 200 nC of charge are involved in the interconversion represented by equation (2). However,

$$Ru^{III}O_x - ne^- \rightleftharpoons Ru^{IV}O_x \qquad (2)$$

unlike conventional redox polymers it is impossible to give a value for D_{ct} for RuO_x, because the concentration of redox centers is not known. The important point is that the magnitude of the maximum generation/collection current is large in comparison to that for the $(BPQ^{2+/+})_n$ system measured in the same way (*vide infra*).

Data for generation/collection experiments for a

$(BPQ^{2+})_n$-coated microelectrode array are presented in Figure 4. The maximum steady-state current passes between generator and collector microelectrodes when the generator electrode potential is more negative than approximately -0.75 V vs. SCE, where $(BPQ^{+})_n$ is reduced, while the collector electrode potential is held at 0.0 V vs. SCE, where $(BPQ^{2+})_n$ is fully oxidized. These data correspond to an array coated with $(BPQ^{2+})_n$ to the extent that ~200 nC of charge are involved in the interconversion represented by equation (3). In comparison to the data for RuO_x-coated

$$(BPQ^{2+})_n + ne^- \rightleftharpoons (BPQ^{+})_n \qquad (3)$$

microelectrodes, Figure 3, the rate of charge transport through $(BPQ^{2+})_n$ is slower as shown by the smaller steady state currents. Slower charge/discharge of the viologen is also found since there is a scan rate dependent generation/collection response. Even at slow scan rates, ~4 mV/s, some of the generated reduced species, $(BPQ^{+})_n$, are also collected by the generator on its return sweep. Thus, the expectation is that the overall current which can pass through a $RuO_x/(BPQ^{2+})_n$ junction will be limited by the rate of charge transport through the $(BPQ^{2+})_n$ polymer, assuming the interfacial charge transport rate, equation (1) and Scheme II, is not limiting.

In characterizing the $(BPQ^{2+})_n$-coated microelectrodes moving the generator more negative than ~-0.8 V vs SCE, the

$(BPQ^0)_n$ state, becomes important, and larger generator/collection currents are observed. The larger currents are expected based on the superior charge transport properties of the $(BPQ^{+/0})_n$ couple compared to the $(BPQ^{2+/+})_n$ couple.[3] Figure 5 shows data giving the relative conductivity of the $(BPQ^{2+/+})_n$ and $(BPQ^{+/0})_n$ states. In the experiment summarized in Figure 5 the relative conductivity is given by the magnitude of the current, I_D, passing between two polymer-connected microelectrodes having a small potential between them, V_D, as a function of the electrochemical potential of the polymer, V_G. Scheme III illustrates the electrochemical system used. Such a system has been referred to as a microelectrochemical transistor and has been used to characterize other redox polymers.[20] The I_D-V_G plot in Figure 5 is in accord with the earlier measurements of the relative conductivity of $(BPQ^{2+/+})_n$ and $(BPQ^{+/0})_n$ coated onto macroscopic electrodes.[3b]

c. Characteristics of $RuO_x/(BPQ^{2+})_n$-based Diodes. Cyclic voltammetry characterization of the modified electrodes of a completed two-terminal microelectrochemical device is shown in Figure 6. Importantly, electrode 1 shows response only to the $(BPQ^{2+/+})_n$ but no electrochemical response to RuO_x. Electrode 2 at the same time shows response to RuO_x but no response to $(BPQ^{2+/+})_n$ on electrode 1. The data in Figure 6 thus establish the desired structure, but the data shown do not establish that there is a connection between electrode 1 and 2 by a $RuO_x/(BPQ^{2+/+})_n$ contact.

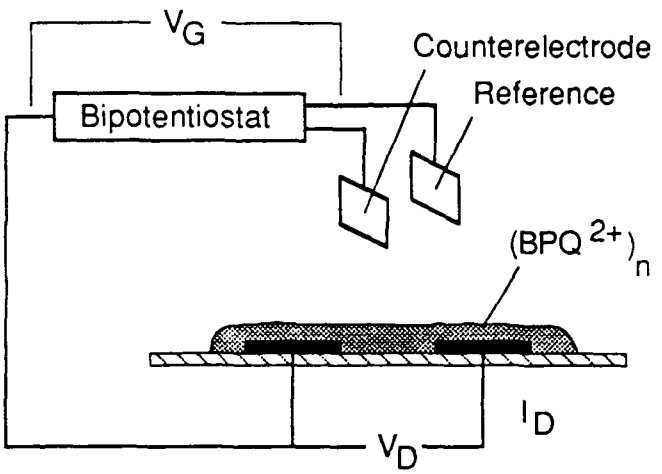

Scheme III. Microelectrochemical system to measure the relative conductivity of $(BPQ^{2+})_n$ redox polymer as a function of electrochemical potential, V_G.

Data that prove electrode 1 and 2 to be connected by a $RuO_x/(BPQ^{2+/+})_n$ contact are summarized in Figure 7. In essence, these data relate to generation/collection experiments like those for RuO_x or $(BPQ^{2+})_n$, Figures 3 and 4, respectively, but in Figure 7 the materials on the generator and collector are different. On the left-hand side of this Figure currents at electrode 1 and 2 are shown, as electrode 2 is held at a potential at which the ratio of $Ru^{III}O_x$ and $Ru^{IV}O_x$ is about one (E_2 = +0.2 V vs. SCE in pH 6 buffer) and electrode 1 is scanned from 0.0 V to -0.8 V vs. SCE. Thus, when the $(BPQ^{2+})_n$ on electrode 1 is reduced to $(BPQ^{+})_n$ a current path between electrode 1 and 2 is possible according to equation (1). On the right-hand side of the figure the experiment is carried out such that electrode 1 is fixed at -0.6 V vs. SCE where the reduced state, $(BPQ^{+})_n$, is significant and electrode 2 is scanned from -0.4 to +0.5 V vs. SCE. Again the currents observed at electrode 1 and 2 are consistent with the redox reaction, equation (1), occurring at the $RuO_x/(BPQ^{2+/+})_n$ interface. The key point is that current between electrode 1 and 2 passes only when the viologen-based polymer is reduced and RuO_x is oxidized. These data prove the connection and show that rectification is expected in a two-terminal device. The relatively low signal to noise in Figure 7 compared to Figures 3 and 4 is due to the facts that only two microelectrodes are used and the spacing between them is ~1.5 μm, not the ~0.1 μm used for experiments summarized by Figures 3 and 4.

The steady-state two terminal current-voltage characteristic of a $RuO_x/(BPQ^{2+/+})_n$-based microelectrochemical device as a function of pH is recorded in Figure 8. These data illustrate that the device can actually pass more steady-state current upon application of potential in one direction than in the other. Current will pass only if the negative lead is connected to electrode 1, reducing the viologen-based polymer to its $(BPQ^+)_n$ state, and the positive lead is connected to electrode 2, oxidizing RuO_x. The electrical cycle is completed through oxidation of $(BPQ^+)_n$ by $Ru^{IV}O_x$, Scheme II. The value of V_T depends on the redox potential difference between the $(BPQ^{2+/+})_n$ and RuO_x. Since the redox potential of RuO_x increases as the pH decreases, as depicted in Figure 1 and Figure 2, V_T of the microelectrochemical diode increases as pH decreases. The inset in Figure 8 is a magnification of the current-voltage characteristic in the region of V_T. The shifts in V_T upon variation of pH correspond roughly to the shifts of $E^{0'}$ for RuO_x in Figure 2. For example, for pH 5.5 the difference between the redox potentials of RuO_x and $(BPQ^{2+/+})_n$ is about 650 mV which is reasonably close to the diode turn-on potential of about 600 mV.

The pH dependent junction between RuO_x and $(BPQ^{2+/+})_n$ can, in principle, be used as a pH sensor, because the current at a fixed applied potential depends on pH in the region of V_T. In Figure 9, current, i, passed through the diode junction held at a constant forward bias of 0.8 V is

shown as a function of time and pH. As the pH of the surrounding electrolyte solution is varied between pH 8.5 and pH 4.5 the current passed through the diode junction rises and falls. The magnitude and direction of current change is consistent with the data presented in Figure 8, which predicts that a diode at 0.8 V forward bias passes more current at a larger pH than at a smaller pH. The qualitative characteristics, V_T and the pH dependence of V_T, of the $RuO_x/(BPQ^{2+})_n$-based diode are in essential accord with expectation.

The magnitude of the current that passes upon forward bias should be discussed. Assuming the redox chemistry at the $RuO_x/(BPQ^{2+})_n$ and redox material/electrode interfaces to be fast, the maximum current is governed by the charge transport properties of the redox materials. Since the $(BPQ^{2+/+})_n$ is the poorer conductor, the current should be limited by this material, not the RuO_x. However, the current found should show a plateau at sufficiently forward bias, and obviously such is not observed, Figure 8. The lack of a plateau signals a role for the $(BPQ^{+/0})_n$ state as the forward bias is increased and this diode characteristic is consistent with the higher conductivity of the $(BPQ^{+/0})_n$ state compared to the $(BPQ^{2+/+})_n$ state, Figure 5. There is an inflection in the current-voltage curve, Figure 8, at a potential consistent with the lower conductivity of the $(BPQ^{2+/+})_n$ state. Even so, the diode current upon forward bias should plateau at sufficiently large bias. However,

the aqueous electrolyte limits the bias to no greater than ~1.2 V, owing to the decomposition potential of H_2O of 1.23 V. Indeed, even reverse bias approaching 1.2 V shows steady current corresponding to onset of the electrolysis of H_2O.

We have made the assumption that charge transport across the $RuO_x/(BPQ^+)_n$ interface is not rate determining, in rationalizing the diode current in Figure 8. This assumption has been verified by preparing the diode shown in Scheme IV. The key result involves comparison of the diode current with and without the hardwire connection between the inner two microelectrodes. With the hardwire connection charge transport across the $Ru^{IV}O_x/(BPQ^+)_n$ interface is not the only mechanism for charge transport. The direct contact of each material with the electrode insures an effective path for current flow in the diode. This scheme of contacts is the same as that used by Murray and co-workers to characterize redox bilayers.[6] We find the same current-voltage properties for the diode with and without the hardwire connection. These reults show that the charge transport rate across the $Ru^{IV}O_x/(BPQ^+)_n$ interface does not limit the diode current.

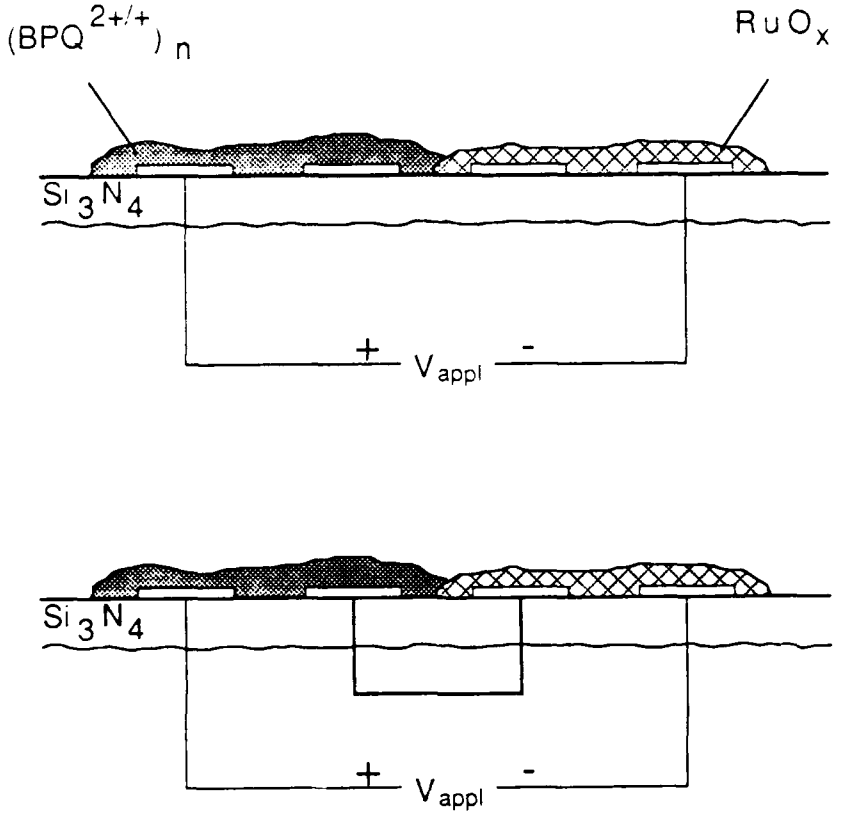

Scheme IV. $RuO_x/(BPQ^{2+})_n$ microelectrochemical diode. Top: without hardwire connection; Bottom: with hardwire connection between the redox materials.

Conclusion

A procedure has been developed to selectively derivatize two adjacent microelectrodes with two different redox materials such that current between the two microelectrodes can only pass when the redox reaction at the $RuO_x/(BPQ^{2+/+})_n$ interface is thermodynamically downhill. Since the redox potential of RuO_x is a function of pH, the current-voltage characteristic of the $(BPQ^{2+/+})_n/RuO_x$ interface is also a function of pH. In principle, the chemically sensitive diode may be useful as a two-terminal electrochemical sensor, because the value of V_T depends on pH in a manner consistent with the pH dependence of the redox potential of the RuO_x. Our results show the viability of rational design and preparation of chemically sensitve microelectrochemical systems based on charge transport properties, thermodynamics, and electrode modification procedures.

Acknowledgements

We thank the Office of Naval Research and the Defense Advanced Research Projects Agency for partial support of this research. MOS would like to thank the Electrochemical Society for a Energy Summer Fellowship Award during a portion of his graduate studies.

REFERENCES

1. Lam, K. W.; Johnson, K. E.; Lee, D. G. *J. Electrochem. Soc.* **1978**, **125**, 1069.
2. Lyons, D. F.; Schloh, M. O.; Hickman, J. J.; Wrighton, M. S. *Chemistry of Materials*, submitted (preceeding article in this issue).
3. (a) Dominey, R. N.; Lewis, T. J.; Wrighton, M. S. *J. Phys. Chem.* **1983**, **87**, 5345; (b) Lewis, T. J.; White, H. S.; Wrighton, M. S. *J. Am. Chem. Soc.* **1984**, **106**, 6947.
4. Kittlesen, G. P.; White, H. S.; Wrighton, M. S. *J. Am. Chem. Soc.* **1985**, **107**, 7373.
5. Schloh, M. O. *J. Electrochem. Soc.* **1989**, **136**, 222C.
6. (a) Pickup, P. G.; Murray, R. W. *J. Electrochem. Soc.* **1984**, **131**, 833; (b) Pickup, P. G.; Kutner, W.; Leidner, C. R.; Murray, R. W. *J. Am. Chem. Soc.* **1984**, **106**, 1991; (c) Denisevich, P.; Willman, K. W.; Murray, R. W. *J. Am. Chem. Soc.* **1981**, **103**, 4727 ; (d) Abruña, H. D.; Denisevich, P.; Umaña, M.; Murray, R. W. *J. Am. Chem. Soc.* **1981**, **103**, 1.
7. Vining, W. J.; Surridge, N. A.; Meyer, T. J. *J. Phys. Chem.* **1986**, **90**, 2281.
8. (a) Smith, D. K.; Tender, L. M.; Lane, G. S.; Licht, S.; Wrighton, M. S. *J. Am. Chem. Soc.* **1989**, **111**, 1099; (b) Hable, C. T.; Cooks, R. M.; Wrighton, M. S. *J. Phys. Chem.* **1989**, **93**, 1190.
9. Chiang, C. K.; Gau, S. C.; Fincher, Jr., C. R.; Park, Y. W.; MacDiarmid, A. G.; Heeger, A. J. *Appl. Phys.*

Lett. **1978**, **33**, 18.

10. Koezuka, H.; Hyodo, K.; MacDiarmid, A. G. *J. Appl. Phys.* **1985**, **58**, 1279.

11. (a) Kaneto, K.; Takeda, S.; Yoshino, K. *Jpn. J. Appl. Phys.* **1985**, **24**, L553; (b) Aizawa, M.; Yamada, T.; Shinohara, H.; Akagi, K.; Shirakawa, H. *J. Chem. Soc, Chem. Commun.* **1986**, 1315; (c) Aizawa, M.; Shinohara, H.; Yamada, T.; Akagi, K.; Shirakawa, H. *Synthetic Metals* **1987**, **18**, 711.

12. Kumar, T. N. Suresh; Contractor, A. Q. *Trans. SAEST* **1986**, **21**, 93.

13. Kanicki, M. *Handbook on Conducting Polymers;* Skotheim, T. J., Ed.; Marcel Dekker: New York, **1986**; p. 544.

14. (a) Kittlesen, G. P.; Wrighton, M. S. *J. Am. Chem. Soc.* **1984**, **106**, 5375; (b) Kittlesen, G. P.; White, H. S.; Wrighton, M. S. *J. Am. Chem. Soc.* **1984**, **106**, 7389; (c) Paul, E. W.; Ricco, A. J.; Wrighton, M. S. *J. Phys. Chem.* **1985**, **89**, 1441; (d) Wrighton, M. S.; Chao, S.; Chyan, O. M.; Jones, E. T. T.; Leventis, N.; Lofton, E. A.; Schloh, M. S.; Shu, C. F. *Chemically Modified Microelectrode Surfaces in Science and Industry;* Leyden, D. E.; Collins, W. T., Eds.; Gordon and Breach: New York, **1987**; p.337.

15. (a)Jones, E. T. T.; Chyan, O. M.; Wrighton, M. S. *J. Am. Chem. Soc.* **1987**, **109**, 5526; (b) Chyan, O. M., Ph.D. Thesis, M.I.T.; **1989**.

16. Rard, J. A. *Chem. Rev.* **1985**, **85**, 1.

17. Burke, L. D.; Healy, J. F. *J.Electroanal. Chem.* **1981, 124**, 327.

18. Burke, L. D.; Lyons, M. E. G. *Modern Aspects in Electrochemistry;* No.18; White, R. E.; Bockris, J. O'M.; Conway, B. E., Eds.; Plenum: New York **1986.**

19. Mallouk, T. E.; Cammarata, V. Crayston, J. A.; Wrighton, M. S. *J. Phys. Chem.* **1986, 90**, 2150.

20. (a) Shu, C.-F.; Wrighton, M. S. *J. Phys. Chem.* **1988, 92**, 5221; (b) Shu, C.-F.; Wrighton, M. S. *ACS Symposium Series*, No. 378; Soriaga, M. P.,Ed.; ACS, Washington, **1988.**

21. (a) Chidsey, C. E.; Feldman, B. J.; Lundgren, C.; Murray, R. W. *Anal. Chem.* **1986, 58**, 601; (b) Feldman, B. J.; Feldberg, S. W.; Murray, R. W. *J. Phys. Chem.* **1987, 91**, 6558.

22. Bard, A. J.; Faulkner, L. R. *Electrochemial Methods;* John Wiley and Sons: New York, **1980.**

FIGURE CAPTIONS

Figure 1. Cyclic voltammetry, 100 mV/s, of a RuO_x-derivatized microelectrode in pH 3.5, 5.5, 7.5, and 8.5 aqueous solution; the buffers used were 1.0 **M** LiCl/0.05 **M** acetate (pH 3.5 and 5.5) and 1.0 **M** LiCl/0.05 **M** Tris buffer (pH 7.5 and 8.5).

Figure 2. Redox potentials, $E^{0'}$, for the RuO_x and the $(BPQ^{2+/+})_n$ redox couple as a function of pH. The redox potentials were determined from cyclic voltammetry in 1.0 **M** NaCl or LiCl electrolyte (0.05 **M** buffer) in H_2O solvent.

Figure 3. Generation/collection cyclic voltammetry of an interdigitated array of close-gap (~0.1 μm) microelectrodes modified with RuO_x in pH 7.5 phosphate buffer as a function of scan rate. The potential of the collector electrodes is held at -0.4 V vs. SCE.

Figure 4. Generation/collection cyclic voltammetry of an interdigitated array of close-gap (~0.1 μm) microelectrodes modified with $(BPQ^{2+})_n$ in 3.0 **M** NaCl electrolyte as a function of scan rate. The potential of the collector electrodes is held at 0.0 V vs. SCE.

Figure 5. I_D vs. V_G for a an array of eight $(BPQ^{2+})_n$-coated microelectrodes.

Figure 6. Cyclic voltammetry of electrode 1 and 2 derivatized with $(BPQ^{2+/+})_n$ and RuO_x as drawn in Scheme I. Note that electrode 1 shows the wave at -0.5 V vs. SCE characteristic of the $(BPQ^{2+/+})_n$ redox couple but no RuO_x electrochemistry, while electrode 2 exhibits only a wave characteristic of RuO_x.

Figure 7. Data establishing that charge can pass through the $(BPQ^{2+/+})_n/RuO_x$ interface. On the left hand side currents observed at electrode 1 and 2 are presented as electrode 2 is held at +0.2 V vs. SCE while electrode 1 is cycled from 0.0 to -0.8 V vs. SCE. The fact that there is current at electrode 2 is consistent with charge transfer through the $(BPQ^{2+/+})_n/RuO_x$ interface. On the right hand side of the figure, current is monitored as electrode 1 is held at -0.6 V vs. SCE and the potential of electrode 2 is cycled from -0.4 to +0.5 V vs. SCE. Again, the observed current is consistent with charge transfer between electrode 1 and 2.

Figure 8. Two-terminal, steady-state current-voltage characteristic of the system drawn in Scheme I. The current-voltage curve shifts to more positive turn-on potentials as pH is decreased. The region of turn-on is expanded in the inset. The shift in turn-on potential with respect to pH change correlates well with the expected

70 mV/pH shift for the RuO_x redox couple.

Figure 9. Current response of a $RuO_x/(BPQ^{2+/+})_n$ diode junction over time as the electrolyte pH is changed between pH 8.5 and pH 4.5. The diode is held at 0.8 V forward bias.

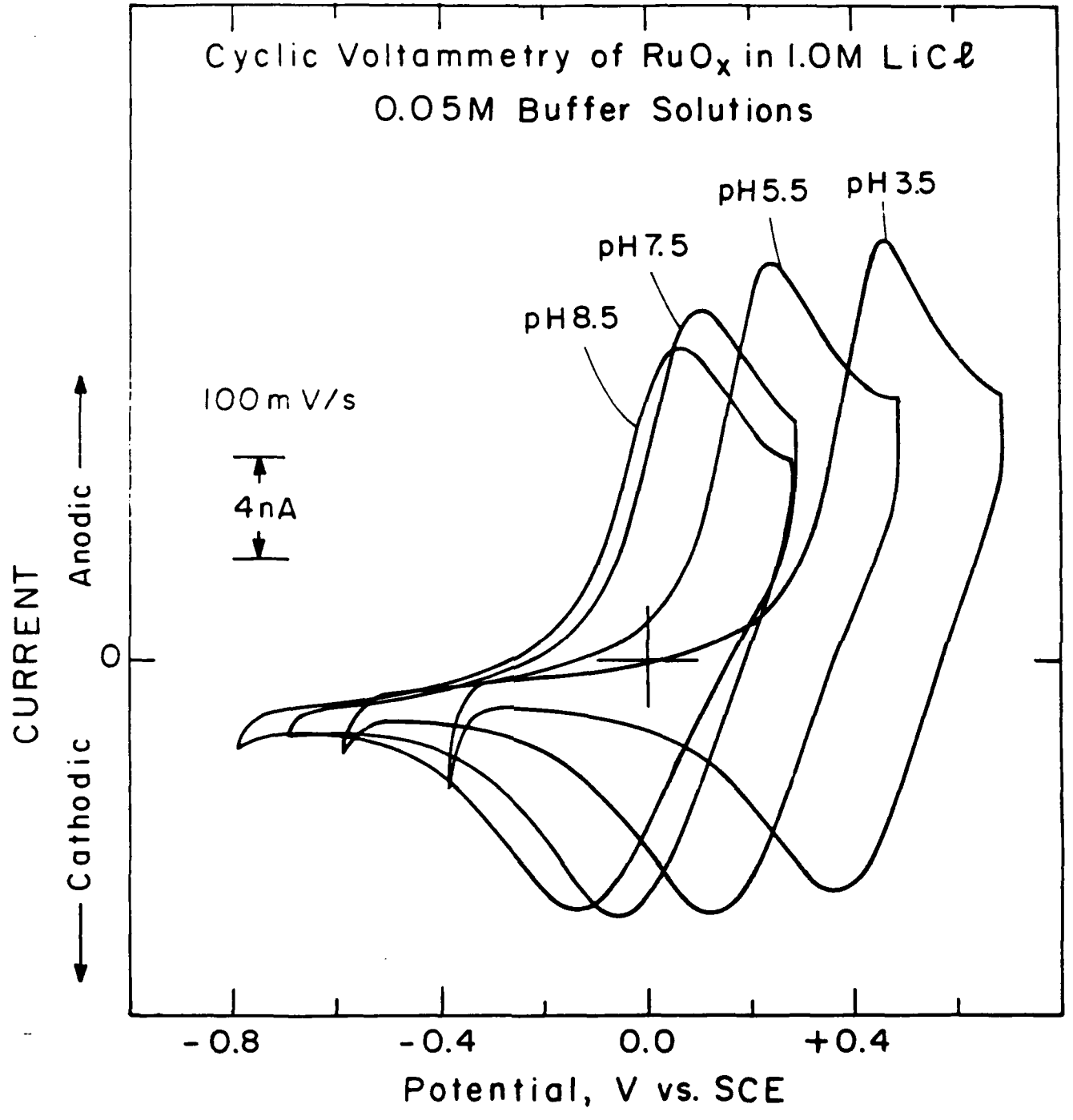
Cyclic Voltammetry of RuO_x in 1.0M LiCl
0.05M Buffer Solutions
pH 3.5
pH 5.5
pH 7.5
pH 8.5
100 mV/s
4nA
CURRENT
Anodic
Cathodic
0
-0.8
-0.4
0.0
+0.4
Potential, V vs. SCE

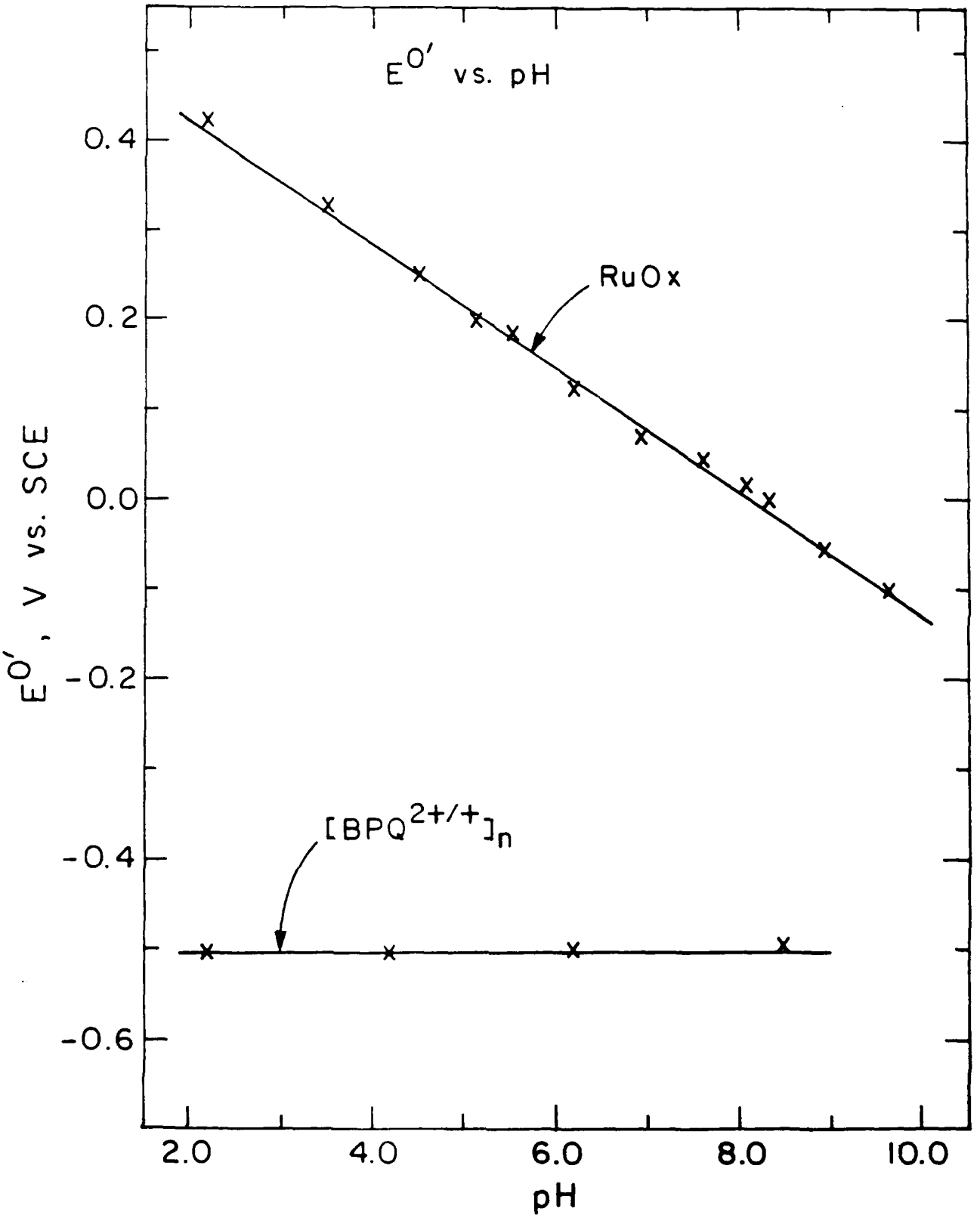
E^0' vs. pH
RuOx
[BPQ^2+/+]n
E^0', V vs. SCE
0.4
0.2
0.0
-0.2
-0.4
-0.6
2.0
4.0
6.0
8.0
10.0
pH

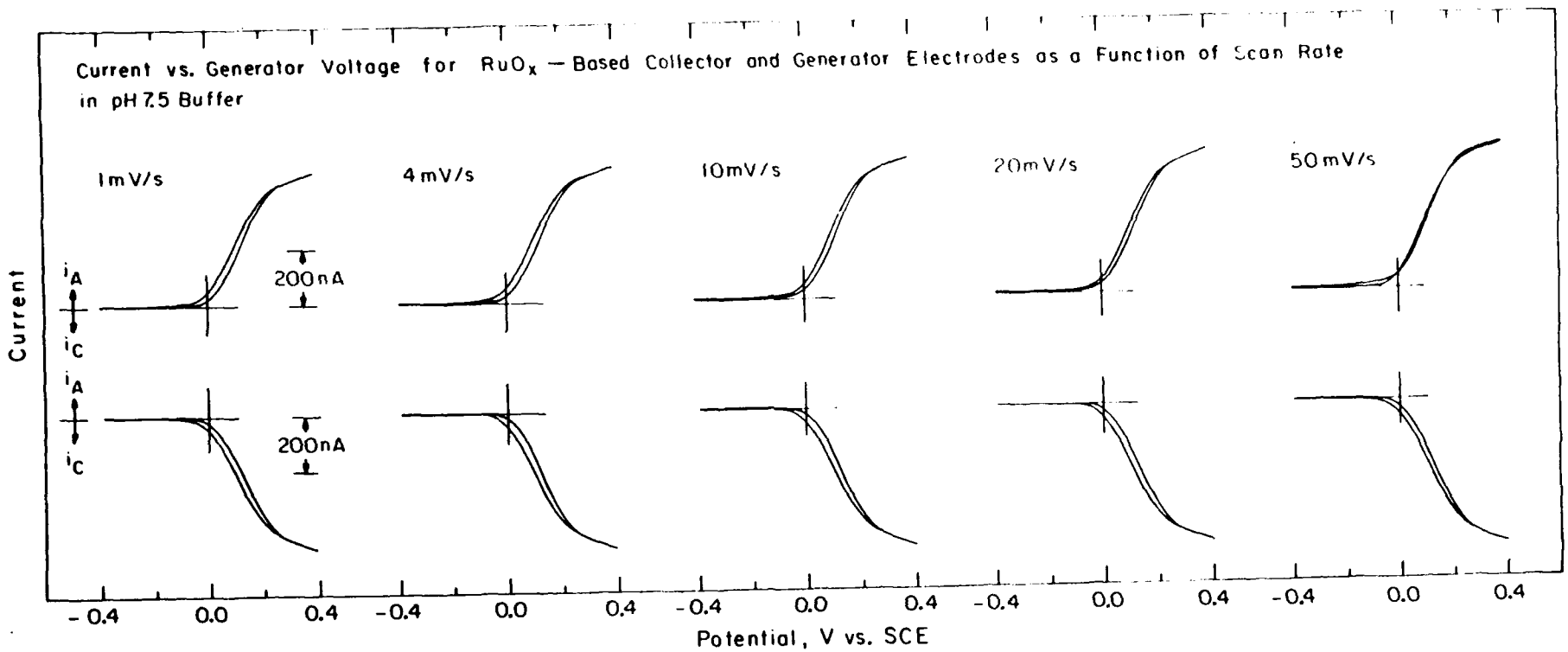
Current vs. Generator Voltage for RuO_x — Based Collector and Generator Electrodes as a Function of Scan Rate in pH 7.5 Buffer
1mV/s
4mV/s
10mV/s
20mV/s
50mV/s
i_A
i_C
200nA
200nA
Current
-0.4
0.0
0.4
Potential, V vs. SCE

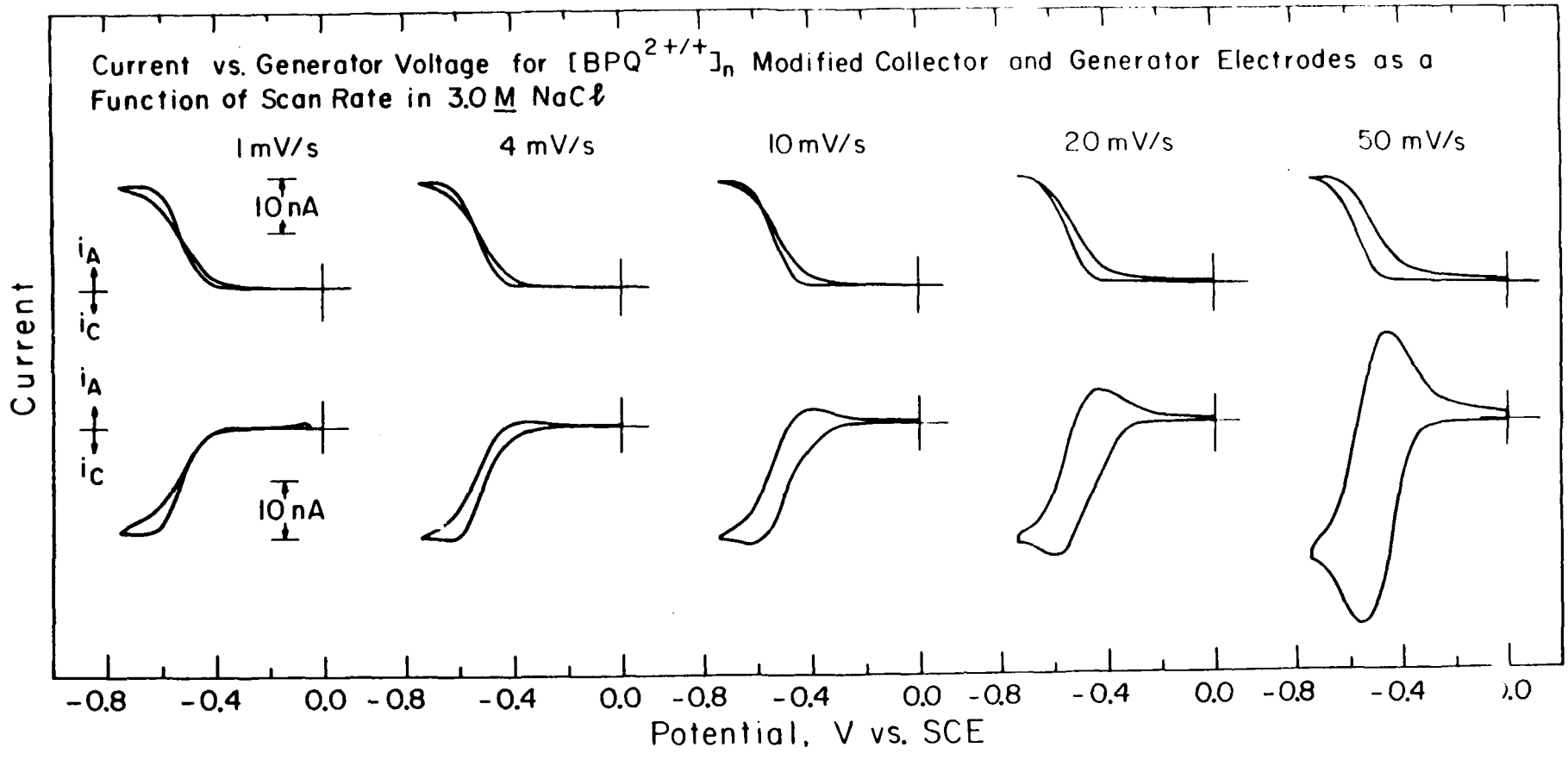
Current vs. Generator Voltage for [BPQ2+/+]n Modified Collector and Generator Electrodes as a Function of Scan Rate in 3.0 M NaCl
1 mV/s
4 mV/s
10 mV/s
20 mV/s
50 mV/s
10 nA
10 nA
iA
iC
iA
iC
Current
-0.8
-0.4
0.0
-0.8
-0.4
0.0
-0.8
-0.4
0.0
-0.8
-0.4
0.0
-0.8
-0.4
Potential, V vs. SCE

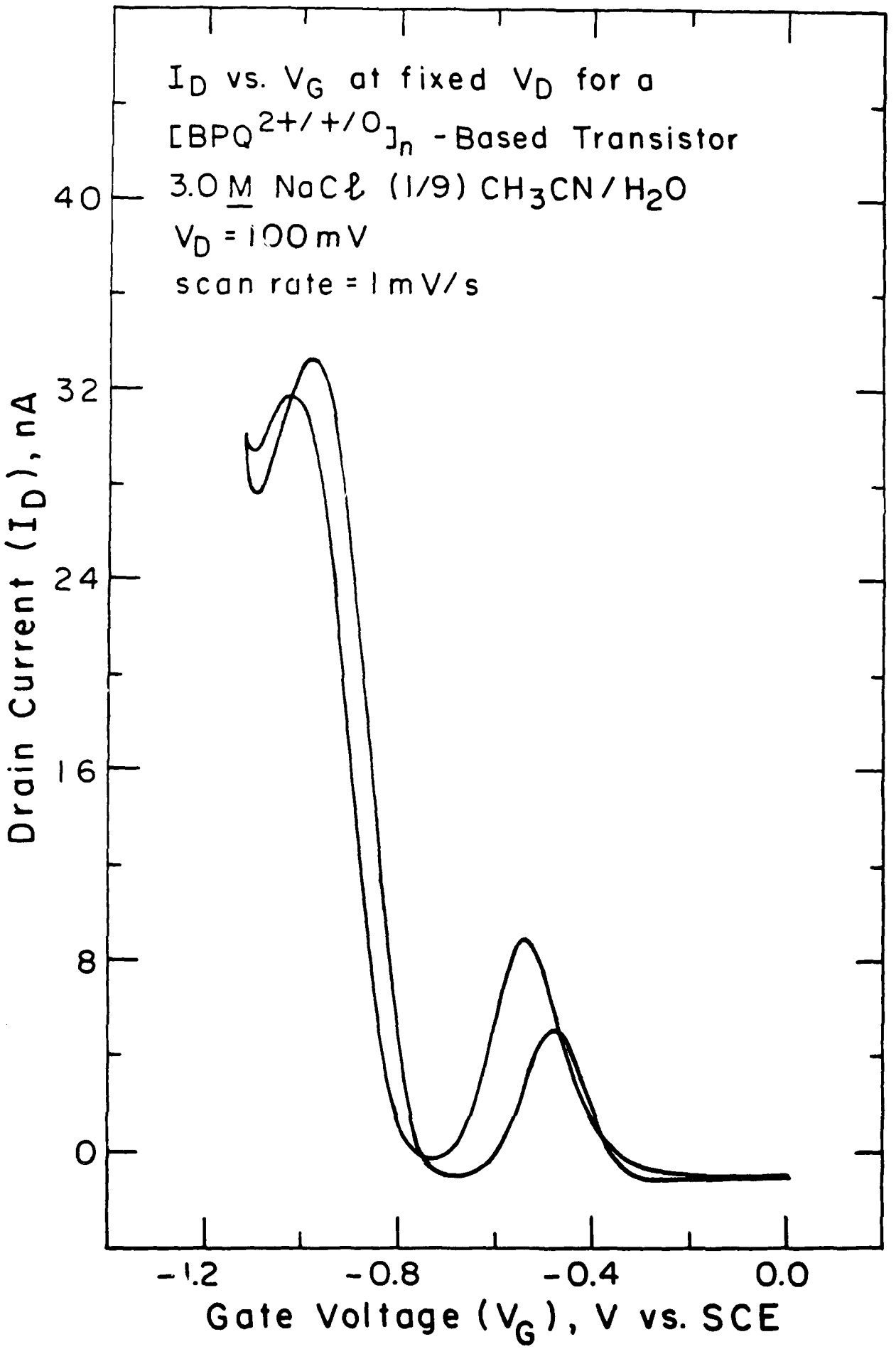
I_D vs. V_G at fixed V_D for a
$[BPQ^{2+/+/0}]_n$ - Based Transistor
3.0 M NaCℓ (1/9) CH_3CN/H_2O
V_D = 100 mV
scan rate = 1 mV/s
Drain Current (I_D), nA
40
32
24
16
8
0
-1.2
-0.8
-0.4
0.0
Gate Voltage (V_G), V vs. SCE

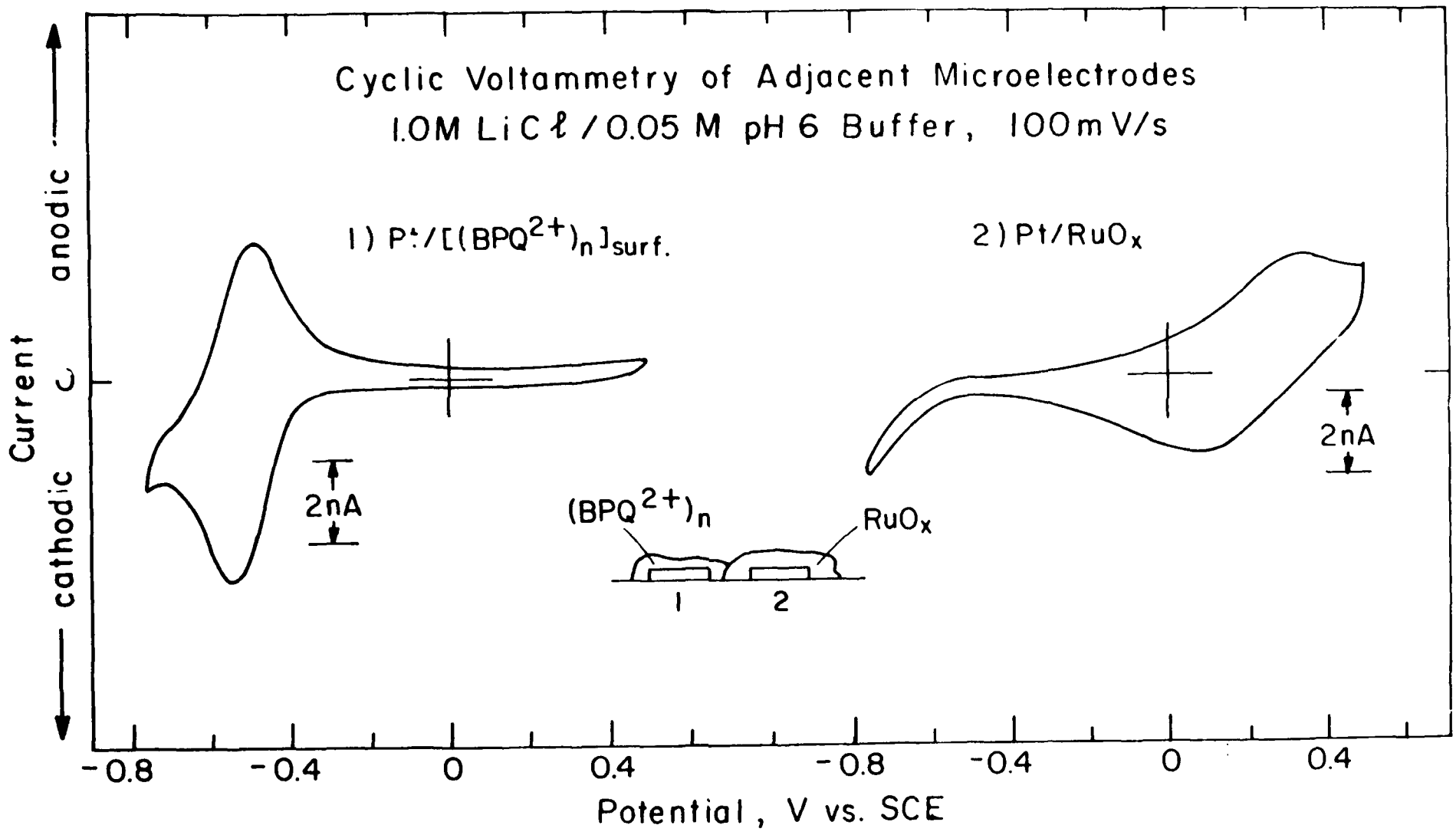
Cyclic Voltammetry of Adjacent Microelectrodes
1.0M LiCl / 0.05 M pH 6 Buffer, 100mV/s
1) Pt/[(BPQ2+)n]surf.
2) Pt/RuOx
Current
anodic
cathodic
2nA
2nA
(BPQ2+)n
RuOx
1
2
-0.8
-0.4
0
0.4
-0.8
-0.4
0
0.4
Potential, V vs. SCE

Redox Processes Mediated at $(BPQ^{2+})_n$ / RuO_x Interface

1.0M LiCl / 0.05 M pH 6 Phosphate Buffer

10 mV/s

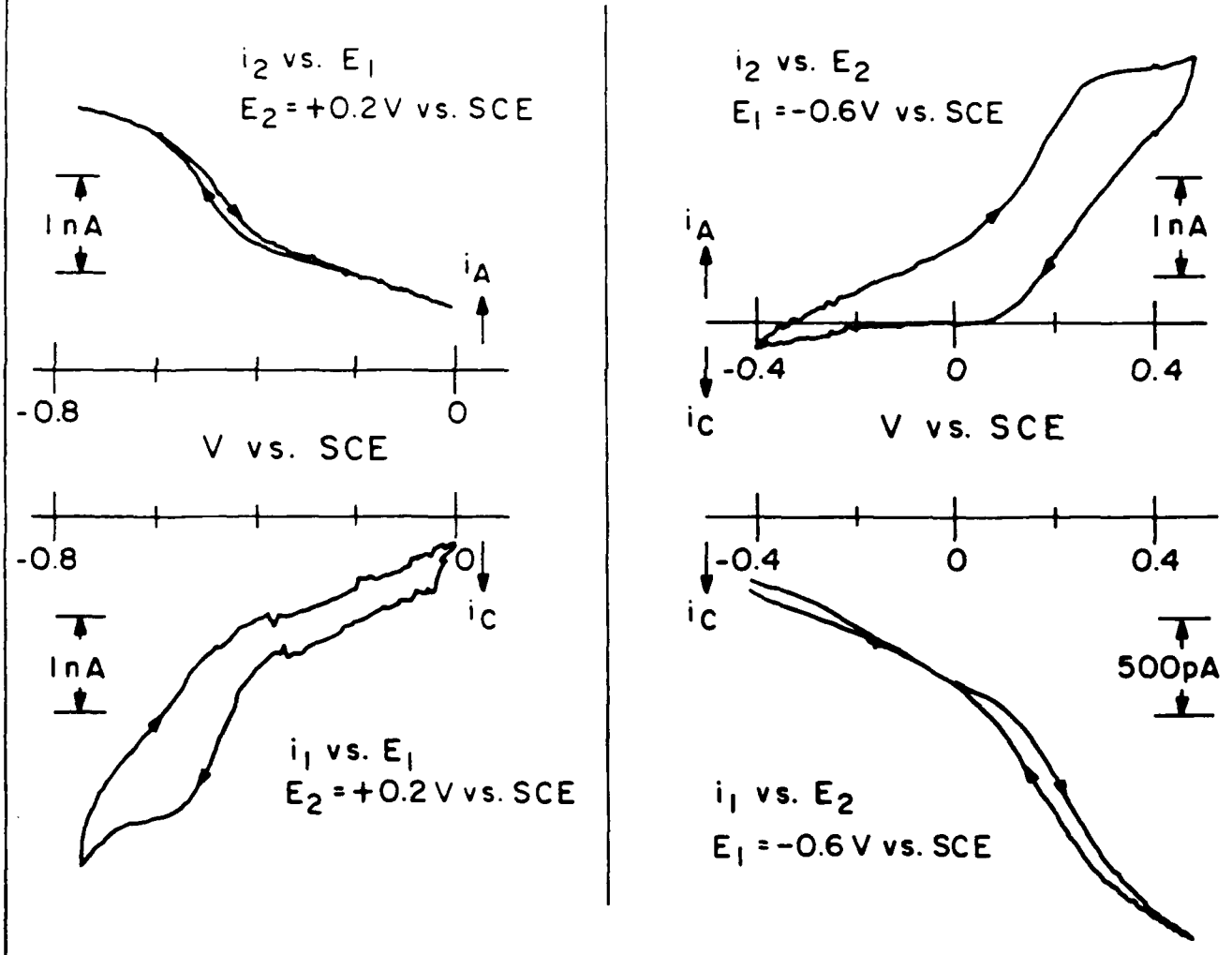

Steady-State Two Terminal i-V Characteristic of $(BPQ^{2+})_n / RuO_x$ Interface as a Function of pH

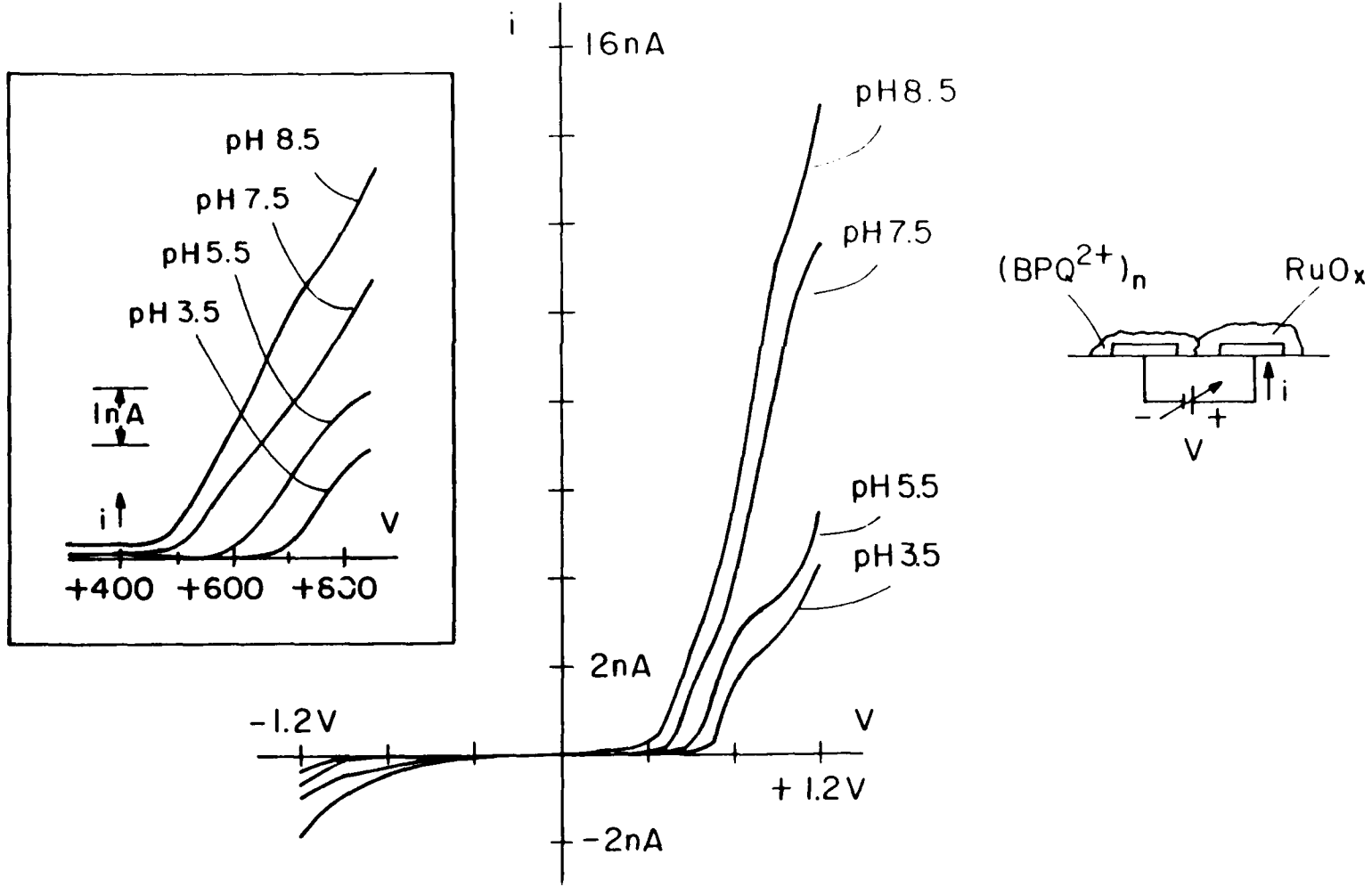

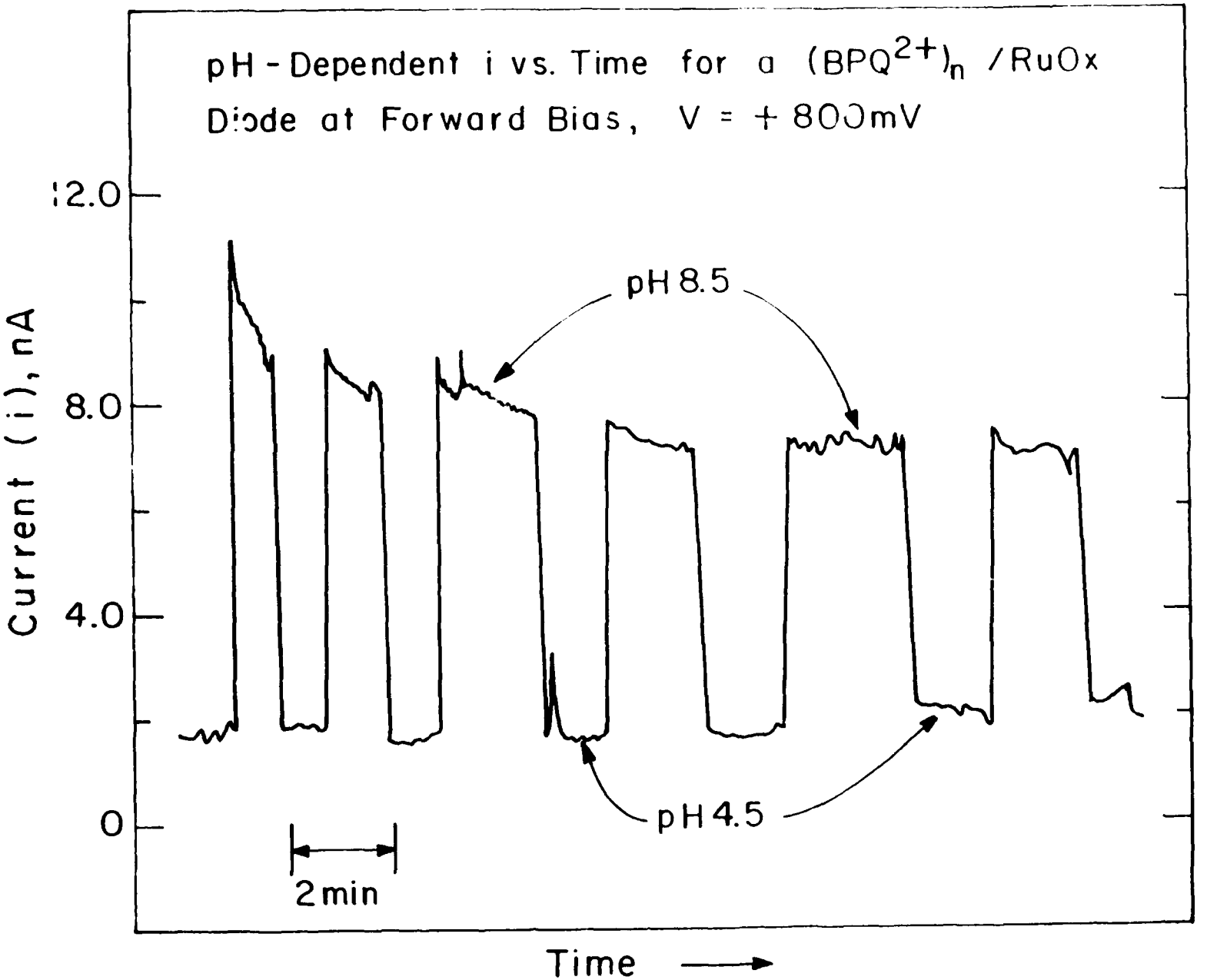
pH - Dependent i vs. Time for a $(BPQ^{2+})_n$ /RuOx
Diode at Forward Bias, V = +800mV
12.0
8.0
4.0
0
Current (i), nA
pH 8.5
pH 4.5
2min
Time

TECHNICAL REPORT DISTRIBUTION LIST - GENERAL

Office of Naval Research (2)
Chemistry Division, Code 1113
800 North Quincy Street
Arlington, Virginia 22217-5000

Dr. Robert Green, Director (1)
Chemistry Division, Code 385
Naval Weapons Center
China Lake, CA 93555-6001

Commanding Officer (1)
Naval Weapons Support Center
Dr. Bernard E. Douda
Crane, Indiana 47522-5050

Chief of Naval Research (1)
Special Assistant for Marine Corps Matters
Code 00MC
800 North Quincy Street
Arlington, VA 22217-5000

Dr. Richard W. Drisko (1)
Naval Civil Engineering Laboratory
Code L52
Port Hueneme, CA 93043

Dr. Bernadette Eichinger (1)
Naval Ship Systems Engineering Station
Code 053
Philadelphia Naval Base
Philadelphia, PA 19112

David Taylor Research Center (1)
Dr. Eugene C. Fischer
Annapolis, MD 21402-5067

Dr. Sachio Yamamoto (1)
Naval Ocean Systems Center
Code 52
San Diego, CA 92152-5000

Dr. James S. Murday (1)
Chemistry Division, Code 6100
Naval Research Laboratory
Washington, D.C. 20375-5000

Dr. Harold H. Singerman (1)
David Taylor Research Center
Code 283
Annapolis, MD 21402-5067

ENCLOSURE(2)